

MICRO ELECTROMECHANICAL SYSTEM (MEMS) VIBRATORY GYROSCOPE WITH PERIODIC COEFFICIENTS: TRANSFER OF ENERGY AND DYNAMIC ANALYSIS AND CONTROL

Nelson José Peruzzi, peruzzi@fcav.unesp.br

Department of Exact Sciences, UNESP – Univ Estadual Paulista, Via de Acesso Prof. Paulo Donato Castellane s/n 14884-900 Jaboticabal - SP, Brazil

Fábio Roberto Chavarette, fabioch@mat.feis.unesp.br

Faculty of Engineering, UNESP – Univ Estadual Paulista, Department of Mathematics, Avenida Brasil, 56, 15385-000, Ilha Solteira, SP, Brazil

José Manoel Balthazar, jmbaltha@rc.unesp.br

UNESP – Univ Estadual Paulista, Department of Statistics, Applied Mathematical and Computation, CP 178, 13500-230, Rio Claro, SP, Brazil

Abstract. *In this paper, we study the dynamics, transfer of energy and control the vibrations of a Micro Electromechanical Systems (MEMS) gyroscope. The MEMS are micro-transducers whose operation is based on elastic and electrostatic forces that convert electrical energy into mechanical energy and vice-versa. These systems can be modeled by 2-DOF spring-mass-damper system and the coupling of the system equations is performed by the Coriolis force. This coupling is responsible for energy transfers of the two vibration modes (drive-mode and sense-mode) and for the resonance in MEMS gyroscope. The model equations have periodic coefficients and as the dimensions of the quantities involved in the system can be inconsistent, it is not advisable, like it is done in literature, the use of perturbation methods for the solution of the system. For this reason, in the analysis and control of MEMS gyroscope we use a technique based on Chebyshev polynomial expansion, the iterative Picard and transformation of Lyapunov-Floquet (LF). For the analysis of the problem, we did the diagram of stability, phase planes and time history of transfer of energy. Finally, we control the MEMS an unstable orbit to a desired periodic orbit.*

Keywords: *Micro Electromechanical system, Non-Linear Dynamics, Control Design, Periodic System, Lyapunov-Floquet transformation.*

1. INTRODUCTION

Micro-electromechanical systems (MEMs) are devices that, even unseen by most, are present in many electronics circuits due to their small mass, high sensitivity and low costs. This technology allows fabrication of electronic components in smaller scale features, hence decreasing amplitudes of motion, but micro-electromechanical devices do not always behave the way one would like them to (Adms,1998) because the devices are small, and the electrical isolation is not perfect, there is some coupling of the actuating drive signal to the sensing capacitors (Turner,1998).

On the other hand, the MEM resonant micro-oscillators have very high natural frequencies and can be operated in nonlinear regime to offer an enhanced performance for device (Shaw and Balachandran, 2008). Thus, the resonant micro-electromechanical oscillators have a great number of applications, mostly, electro-mechanical filters, biological and chemical sensing, force sensing, scanning probe microscopes and sensors, like gyroscope and accelerometer.

Recently, have been developed vibratory micro-electromechanical gyroscopes that separate oscillation modes for drive (actuation) and sense (detection). The drive mode is based on variable force actuators that depend on the force-time variation relation and in the sense mode the response is measured and calibrated with the rotation rate.

Vibrating MEMGyroscopes is based on the energy transferred on the coupling of two resonant modes from the Coriolis force. Such devices employ a proof mass constrained to move in a plane with two orthogonal resonant modes. The two modes are coupled only by the rotation of the gyroscope about the normal vector to displacement plan of modes. High rate sensitivity for such devices requires high resonance quality and matched modal frequencies for the two orthogonal modes (Yazdi, 1998).

The design requirements such as orthogonality and frequency matching are not generally robust under parameter uncertainty. Frequency misalignment causes substantial decrease in rate sensitivity, and model misalignment causes erroneous rate measurement (Miller, 2008).

The analysis of the dynamic of the MEMGyroscopes has been showing that the sensitivity those devices improve as the frequency mismatch between the two modes decreases. Moreover, the mechanical coupling between drive mode and sense mode makes the dynamic of the system unstable (Mochida, 1999).

Application of some nonlinear effects on system can be used to alter, significantly, the behavior dynamic of the MEMGyroscopes. The idea is to separate the drive and sense signals by parametrically exciting the device far from its

natural frequency. This is only possible in systems governed by Mathieu-type equations, due to the unique way energy is transferred during parametric excitation (Turner, 1998).

Zhang (Zhang, 2002) reports the effects of nonlinearity on the behavior of parametric resonance of a 2-DOF MEM vibratory gyroscope. In this 2-DOF system, the drive-mode consists of a 1-DOF oscillator governed by a nonlinear Mathieu equation and the sense-mode is a 1-DOF oscillator governed by a Duffing equation, both of them coupled by the Coriolis force.

The nonlinear Mathieu equation is the simplest second order nonlinear differential equation with periodic coefficients that describes the parametric excitations. Thus, in this system can produce large responses even if the excitation frequency is far away from the natural frequency (Nayfeh, 1979). Moreover, in the case of the second-order system with time periodic coefficients, the dynamics a parametrically driven oscillator, the sensitivity depends on the transition between zero and large response and the transition can be very sharp (Oropeza-Ramos, 2005).

In order to achieve high sensitivity, the drive and the sense resonant frequencies are typically designed and tuned to match, and the device could be controlled for the dynamic oscillate at or near the peak of the response curve. (Oropeza-Ramos, 2008)

The solution analysis of the 2-DOF MEM vibratory gyroscope, traditionally, was examined in term of perturbation method (Oropeza-Ramos, 2008; Zhang, 2002). Due to small quantities of magnitudes that are involved in the problem, especially when these quantities are coefficients of periodic terms, we analyze the problem from the Lyapunov-Floquet theorem.

This work, we study the dynamic of the 2-DOF MEM vibratory gyroscope by analysis of the Floquet multiplier of the approximate fundamental solution matrix of the 2-DOF periodic system. The technique used on approximation employs both Picard interaction and expansion in shifted Chebyshev polynomials (Sinha, 1997; Peruzzi, 2006). Moreover, we obtain the Stability diagram for the control parameters voltage e frequency where were determine the bifurcations Fold, Hopf and Flip. For a values set of control parameters unstable, the dynamics of the system was subsequently studied and controlled to a desired periodic orbit, by a states feedback control technique based on Lyapunov-Floquet transformation.

2. MEMGYROSCOPE MODEL

On MEMGyroscope the energy transferred on the coupling of two resonant modes. Thus, a vibratory micro-gyroscope can be modeled as two independent spring-mass-damper oscillators coupled by Coriolis force. The physical model (Fig. 1), shows the proof-mass is suspended by a set of springs that allow oscillations in two orthogonal directions and the angular rotation Ω_z about z -axis (Oropeza-Ramos, 2005).

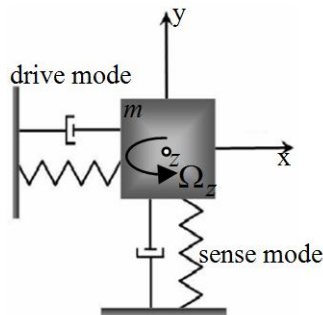


Figure 1. Physical model of a 2-DOF vibratory gyroscope

The governing equations of this 2-DOF system in the drive mode (x-direction) and sense mode (y-direction) were modeled mathematically in (Oropeza-Ramos, 2007) as:

$$\begin{cases} m\ddot{x} + c_x\dot{x} + F_r(x) = F_a(x, t^*) + 2m\Omega_z\dot{y} \\ m\ddot{y} + c_y\dot{y} + F_r(y) = -2m\Omega_z\dot{x} \end{cases} \quad (1)$$

where, m represents the mass of the shuttle, c_x and the damping coefficient of oscillator in the x -direction, c_y the damping coefficient of oscillator in the y -direction. $F_r(x)$ represents the elastic restoring force from the springs drive mode and $F_r(y)$ the elastic restoring force drive sense. $F_a(x, t^*)$ is the actuation force and 2-DOF is coupled by terms $2m\Omega_z\dot{y}$ and $2m\Omega_z\dot{x}$ which represent the rotation-induced Coriolis forces.

The restoring forces $F_r(x)$ and $F_r(y)$ were modeled as:

$$F_r(x) = k_{x1}x + k_{x3}x^3 \quad \text{and} \quad F_r(y) = k_{y1}y + k_{y3}y^3 \quad (2)$$

where, k_{x1} and k_{y1} are linear stiffness coefficients and k_{x3} and k_{y3} are cubic stiffness coefficients for drive and sense modes.

In order to generate a parametric resonance response, the actuation force is defined by:

$$F_a(x, t^*) = -(r_1x + r_3x^3)V^2(t^*) \quad (3)$$

where, r_1 and r_3 are linear and cubic electrostatic stiffness, respectively. The voltage applied on system is $V(t^*) = V_A \sqrt{1 + \cos(\omega t^*)}$, where V_A is the input voltage amplitude and ω is the actuation frequency.

Substituting (2) and (3) in the equation (1), rescaling the time variable by $2\tau = \omega t^*$ and considering dimensionless parameters (Oropeza-Ramos, 2007): $\alpha_x = \frac{2c_x}{m\omega}$; $\alpha_y = \frac{2c_y}{m\omega}$; $\beta_{x1} = \frac{2r_1V_A^2}{m\omega^2}$; $\beta_{x3} = \frac{2r_3V_A^2}{m\omega^2}$; $\delta_{x1} = \frac{4(k_{x1} + r_1V_A^2)}{m\omega^2}$;

$\delta_{x3} = \frac{4(k_{x3} + r_3V_A^2)}{m\omega^2}$; $\delta_{y1} = \frac{4k_{y1}}{m\omega^2}$; $\delta_{y3} = \frac{4k_{y3}}{m\omega^2}$; $\gamma = \frac{4\Omega_z}{\omega}$, we can write the dimensionless equations of motion of the MEMGyroscope as:

$$\begin{cases} x'' = -\alpha_x x' - (\delta_{x1} + 2\beta_{x1} \cos(2\tau))x - (\delta_{x3} + 2\beta_{x3} \cos(2\tau))x^3 + \gamma y' \\ y'' = -\alpha_y y' - \delta_{y1}y - \delta_{y3}y^3 - \gamma x' \end{cases} \quad (4)$$

where, $(\cdot)' = \frac{d(\cdot)}{d\tau}$.

Note that, first equation of the dimensionless system (4) is nonlinear Mathieu-type equation and the second is Duffing equation. Since it is not possible to obtain an exact closed form solution of the nonlinear Mathieu equation (Oropeza-Ramos, 2009), the stability analysis of the solutions of the nonlinear periodic system (4) has been examined numerically in term of transition curves that define the boundaries of instability regions.

The method that was used for analysis and control of 2-DOF vibratory micro gyroscope is based on L-F transformation (Lyapunov-Floquet transformation), the Chebyshev polynomial expansion and the Picard iterative method (Sinha, 1997 and 2000; Peruzzi, 2005 and 2006).

According to (Nayfeh, 1979) the first-order parametric resonance for a linear Mathieu equation, occurs when the driving frequency is near twice the natural frequency of the system $\omega \cong 2\omega_0$. Thus, we take as control parameters the voltage (V_A) and the actuation frequency (ω).

On numerical simulation of the system (4), we used $m = 1.4e-8$ Kg, $\omega_0 = 26.48$ KHz and we considered the nondimensional parameters:

$$\begin{aligned} \alpha_x &= 1.5e-3; \alpha_y = 1.5e-3; \beta_{x1} = -1.01e-2; \beta_{x3} = -8.75e-4; \delta_{x1} = 1.01; \\ \delta_{x3} &= 5.1e-3; \delta_{y1} = 1.11; \delta_{y3} = 0.0123; \gamma = 0.017 \end{aligned} \quad (5)$$

In numerical simulations were implemented in Matlab® 6.1 (The Mathworks, Inc., 2001, USA). We used Chebyshev polynomials of the first kind modified with grade 20 and 40 Picard interactions, as in (Peruzzi, 2005 and 2006).

3. NUMERICAL SIMULATIONS RESULTS AND DYNAMICS ANALYSIS

Figure 2 (a,b) shows drive and sense modes dynamic of the vibratory MEMGyroscope for the control parameters $V_A = 20V$ and $\omega = 52KHz$, ie, the system was driving near of the parametric resonance. The Floquet multiplier are $\mu_{1,2} = -0.9957 \pm 0.0615i$, $\mu_3 = -1.0097$ and $\mu_4 = -0.9857$. As the magnitude of the four Floquet multipliers is next to 1 ($|\mu_{1,2}| = 0.9977$, $|\mu_3| = 1.0097$ and $|\mu_4| = 0.9857$) the system is operating on bifurcation boundaries.

This can be observed transient response part of the Fig. 2(a,b). Both drive and sense modes are showing unstable exponential growth before of stable periodic orbit. Figures 3(a,b) present transfer energy between drive and sense

modes due to Coriolis force. Observe in the Fig. 3b (zoom of the marked area) the intensive transfer of energy between the vibration modes, mainly, in the transient part.

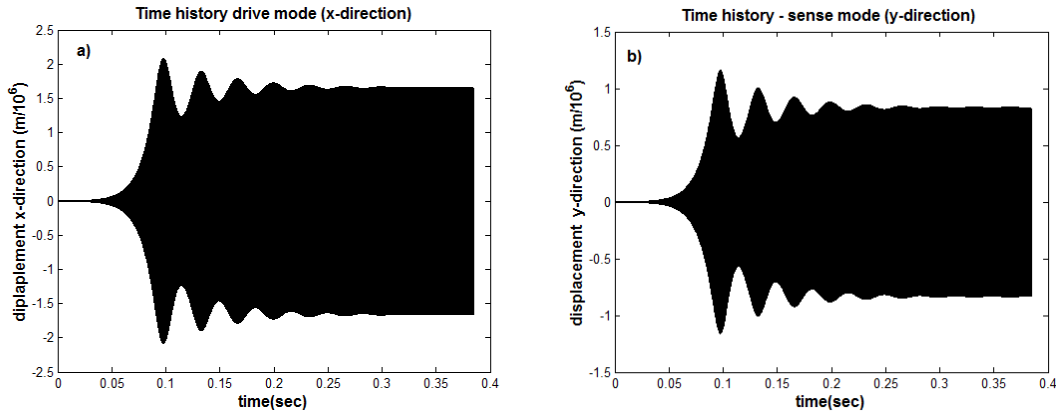


Figure 2. Time history a) drive mode, and b) sense mode.

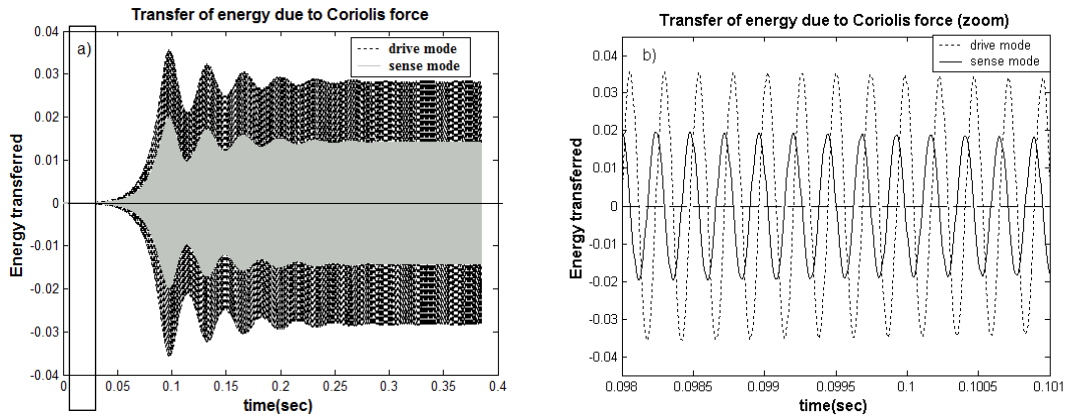


Figure 3. a) time history of the transfer of energy between drive and sense modes due to Coriolis force; b) zoom of the marked area.

To better understand the behavior of the dynamics of vibratory MEMGyroscope we obtain the stability diagram for control parameters the voltage (V_A) and the actuation frequency ω . To this, must be found the values in the plane $(\omega - V_A) \in R^2$ that make the critic system, ie, the voltage (V_A) and frequency (ω) values for which Floquet multipliers have magnitude 1.

For the control parameters $5 \leq V_A \leq 60$ (Volts), $1 \leq \omega \leq 55$ (KHz) and considering the values parameters (5), we obtain the stability diagram in the Fig. 4. In the plane $(\omega - V_A)$, we can be observed the bifurcation boundaries (Flip, Fold and Hopf) of the vibratory micro gyroscope.

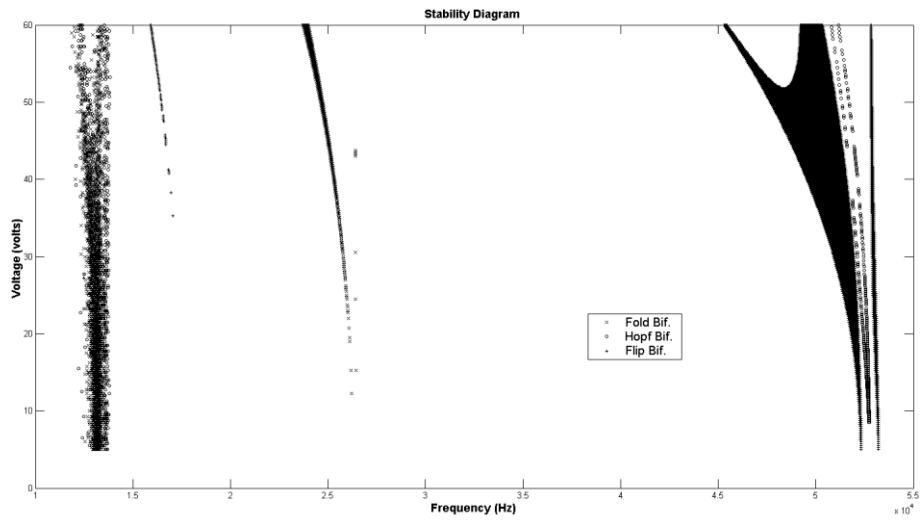


Figure 4. Stability diagram of the MEMGyroscope.

Figures 5(a,b) show the chaotic dynamic ($\lambda_1=0.05$) of Lyapunov exponent of the MEMGyroscope and zoom of the marked area.

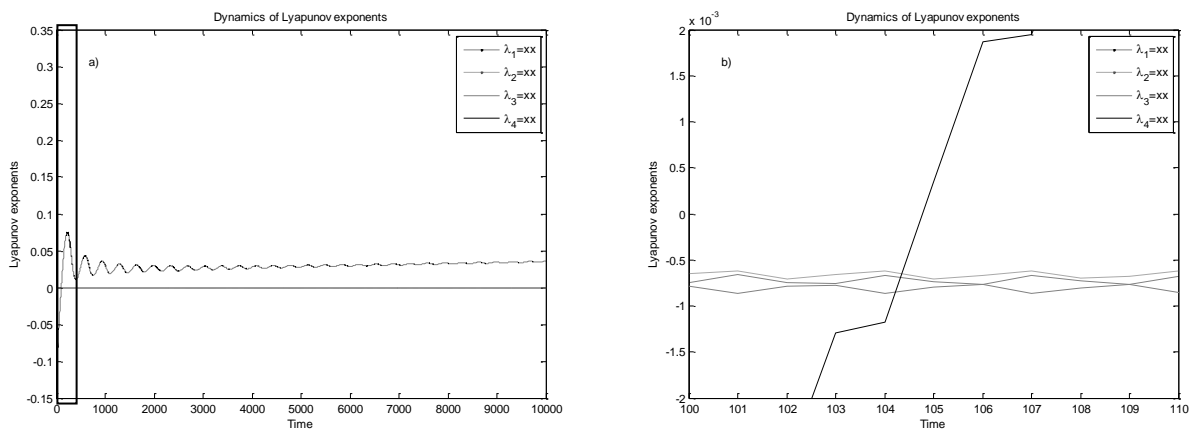


Figure 5. a) Dynamics of Lyapunov exponents of the MEMGyroscope, and b) Zoom of the Lyapunov exponents.

4. CONTROL DESIGN BASED ON SINHA'S THEORY

Considerer the controlled vibratory MEMGyroscope obtained from equation (4).

$$\begin{cases} x'' = -\alpha_x x' - (\delta_{x_1} + 2\beta_{x_1} \cos(2\tau))x - (\delta_{x_3} + 2\beta_{x_3} \cos(2\tau))x^3 + \gamma y' + u_1 \\ y'' = -\alpha_y y' - \delta_{y_1} y - \delta_{y_3} y^3 - \gamma x' + u_2 \end{cases} \quad (6)$$

where, u_1 and u_2 are linear state control laws (Sinha, 1994, 1997 and 2000).

The term of control $u(\tau) = [u_1(\tau) \quad u_2(\tau)]^T$ is defined as:

$$u_i(\tau) = u_{f_i} + u_{t_i}, \quad i = 1, 2 \quad (7)$$

where,

$$u_{f_i} = \begin{cases} u_{f_1} = \ddot{x} - f_1(\tau, x(\tau), \dot{x}(\tau), \dot{y}(\tau)) \\ u_{f_2} = \ddot{y} - f_2(\tau, y(\tau), \dot{y}(\tau), \dot{x}(\tau)) \end{cases} \quad (8)$$

are feedforward part of the control law, and:

$$\begin{cases} u_{t_1} = -F_1(\tau)(x - x_d) \\ u_{t_1} = -F_2(\tau)(x - x_d) \end{cases} \quad (9)$$

are states feedback where $F_i(t)$ was defined in (Sinha,1994) as $F_i(t) = B^*(t)Q(t)\bar{k}Q^{-1}(t)$.

Figures 6 and 7 (a,b) present the time history and phase plane for simulations of the non-controlled vibratory MEMGyroscope (6) when $u_1 = u_2 = 0$, $V_A = 50V$ and $\omega = 50\text{ KHz}$. Observe that both drive and sense modes dynamics are unstable. Note that, in the Fig. 5, the displacement amplitudes are increasing in the time and, in the Fig. 7, we can see unstable orbits.

In fact, the Floquet multipliers of the system (6) are $\mu_{1,2} = -0.9819 \pm 0.1758i$, $\mu_3 = -1.1018$ and $\mu_4 = 0.9032$. The magnitude of the multiplier $|\mu_3| = 1.1018$ confirms the instability of the system (6) for these set of parameters values.

The strategy of linear control proposed in (7) can be used to control the instabilities of the vibratory micro gyroscope. In this control design the objective is conduct the unstable orbit to a desired periodic orbit applying the Lyapunov-Foquet transformation. The desired orbits, for control design to drive and sense modes, are the simple

$\left(\frac{2\pi}{a}\right)$ -periodic:

$$\begin{cases} x_d = A\cos(a\tau) + B\sin(a\tau) \\ y_d = C\sin(a\tau) + D\cos(a\tau) \end{cases} \quad (10)$$

whith A, B, C, D and $a \in R$.

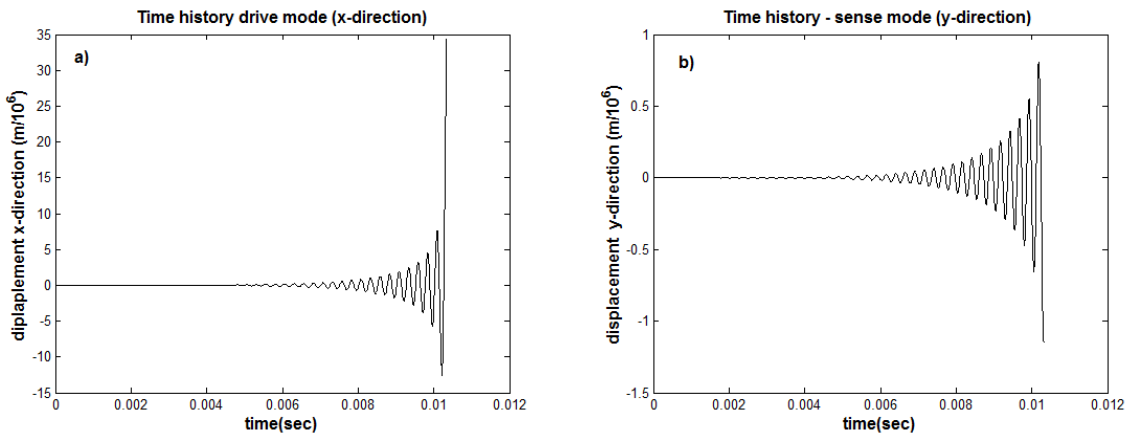


Figure 6. Time history for non-controlled MEMGyros. a) drive mode, and b) sense mode

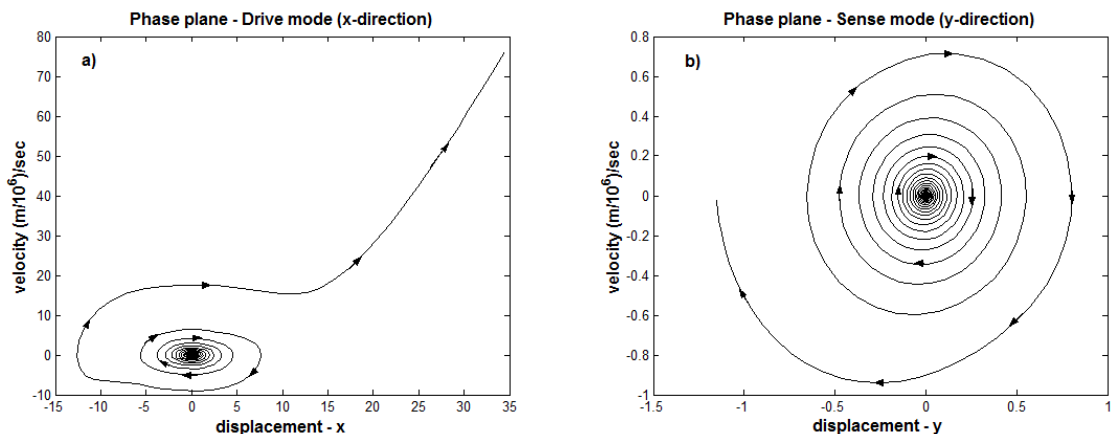


Figure 7. Phase plane for non-controlled MEMGyros. a) drive mode, and b) sense mode

Substituting the equation (10) in (8) and the result in (6), we determine the dynamic error between the drive mode trajectory $x(\tau)$ and desired one ($x_d(\tau)$, $e_x = x(\tau) - x_d(\tau)$), and sense mode trajectory $y(\tau)$ and $y_d(\tau)$, ($e_y = y(\tau) - y_d(\tau)$).

Thus, the dynamic error between the systems (6) and (10) can be written as:

$$\begin{cases} \ddot{e}_x = -(E_1 + E_2 + E_3)e_x - \alpha_x \dot{e}_x + \gamma \dot{e}_y + u_{t1} \\ \ddot{e}_y = -(E_4)e_y - \alpha_y \dot{e}_y - \gamma \dot{e}_x + u_{t2} \end{cases} \quad (11)$$

where, $E_1 = 2\beta_x \cos(2\tau)$; $E_2 = \delta_x + 3\delta_{x3} \left[\frac{A^2 + B^2}{2} + \frac{A^2 - B^2}{2} \cos(2a\tau) + AB \sin(2a\tau) \right]$ and

$$E_3 = 6\beta_{x3} \left[\frac{A^2 + B^2}{2} \cos(2\tau) + \frac{(A^2 - B^2) \cos(2(a+1)\tau) + 2AB \sin(2(a+1)\tau)}{4} + \frac{(A^2 - B^2) \cos(2(a-1)\tau) + 2AB \sin(2(a-1)\tau)}{4} \right]$$

Considering $A=2$, $B=1$, $C=1$, $B=1$ and $a=1$

$$\begin{cases} \ddot{e}_x = - \left[\delta_x + \frac{15\delta_{x3}}{2} + \frac{9\beta_{x3}}{2} \right] + \left(2\beta_x + 15\beta_{x3} + \frac{9\delta_{x3}}{2} \right) \cos(2\tau) + 6\delta_{x3} \sin(2\tau) \\ \quad + \frac{9\beta_{x3} \cos(4\tau)}{2} + 6\beta_{x3} \sin(4\tau) e_x - \alpha_x \dot{e}_x + \gamma \dot{e}_y + u_{t1} \\ \ddot{e}_y = -(\delta_y + 3\delta_{y3} [1 + \sin(2\tau)]) e_y - \alpha_y \dot{e}_y - \gamma \dot{e}_x + u_{t2} \end{cases} \quad (12)$$

Changing the variables $e_x = z_1$; $e_y = z_2$; $\dot{e}_x = z_3$, $\dot{e}_y = z_4$ and $t = T\tau$ we can rewrite the nonlinear equation (12) in the linearized space-state form, on principal period $T = 2\pi$, as:

$$\begin{bmatrix} \dot{z}_1 \\ \dot{z}_2 \\ \dot{z}_3 \\ \dot{z}_4 \end{bmatrix} = [\bar{A}(V_A, \omega)] \begin{bmatrix} z_1 \\ z_2 \\ z_3 \\ z_4 \end{bmatrix} + \begin{bmatrix} 0 & 0 \\ 0 & 0 \\ 1 & 0 \\ 0 & 1 \end{bmatrix} \begin{bmatrix} u_{t1} \\ u_{t2} \end{bmatrix} \quad (13)$$

where, $\bar{A}(V_A, \omega) = T[A_0 + A_1 \cos(2\pi t) + A_2 \sin(2\pi t) + A_3 \cos(4\pi t) + A_4 \sin(4\pi t)]$, $t \in [0,1]$. The matrix A_0, \dots, A_4 are defined on appendix A.

The states transition matrix of (13), calculated in the end of period T , was obtained numerically as:

$$\phi(T) = \begin{bmatrix} -1.0139 & -0.0277 & -0.1043 & 0.0061 \\ 0.0233 & -1.0003 & 0.0056 & -0.3155 \\ -0.2464 & 0.001 & -1.006 & -0.0271 \\ 0.0014 & 0.2873 & 0.02814 & -0.9034 \end{bmatrix} \quad (14)$$

The Floquet multipliers of the system (14) are $\mu_{1,2} = -0.9518 \pm 0.2983i$, $\mu_3 = -1.1683$ and $\mu_4 = 0.8517$. The magnitude of the multiplier $|\mu_3| = 1.1683$ shows that (13) still unstable the set of parameters values.

Applying the Lyapunov-Floquet transformation ($z(t) = Q(t)q(t)$, where $Q(t) = \phi(T)e^{-Rt}$) in the equation (13) we obtain the equivalent system:

$$\dot{q}(t) = \begin{bmatrix} 0.0004 & 0.0087 & 0.0331 & 0.0001 \\ -0.0071 & 0.0149 & 0.0001 & 0.1022 \\ 0.0783 & -0.0001 & -0.002 & 0.0088 \\ -0.0003 & -0.0931 & -0.00933 & -0.0164 \end{bmatrix} q(t) + Q^{-1}(t) \begin{bmatrix} 0 & 0 \\ 0 & 0 \\ 1 & 0 \\ 0 & 1 \end{bmatrix} \begin{bmatrix} u_{t1} \\ u_{t2} \end{bmatrix} \quad (15)$$

Note that the linear part is time invariant and the eigenvalues are: $-0.0007 \pm 0.0967i$, 0.04951 and -0.0511 . The presence of 0.04951 indicates the instability of (15). Applying the pole placement technique is possible to obtain the state feedback part $u_i(t)$.

Considering the new poles of (15): $-2, -1, -2, -1$; we could calculate, numerically, the time invariant gain matrix (Sinha, 2000):

$$\bar{K} = \begin{bmatrix} 4.3717 & 0.0847 & 0.5202 & 0.0122 \\ 0.0515 & 4.2546 & -0.0092 & 1.5581 \\ -61.93 & -1.522 & -7.368 & -0.2916 \\ -0.6519 & -19.8153 & -0.006 & -7.2549 \end{bmatrix} \quad (16)$$

Thus, the control law $u(\tau) = [u_1(\tau) \ u_2(\tau)]^T$ can be used to control a vibratory MEMGyroscope (6) to the desired periodic orbit (10).

Figure 8(a,b) present the time history of the controlled vibratory MEMGyroscope (6) for $V_A = 50V$ and $\omega = 50KHz$. Observe that both drive and sense modes dynamics are stable periodic orbit. The phase plane to the controlled system and the desired orbits are show in Fig. 9(a,b). Note that control design was successful.

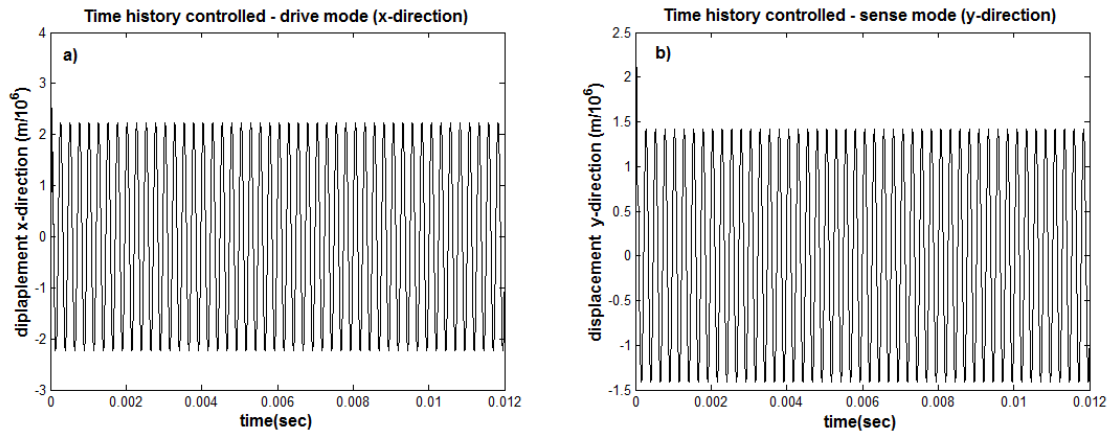


Figure 8. Time history for controlled MEMGyros. a) drive mode, and b) sense mode

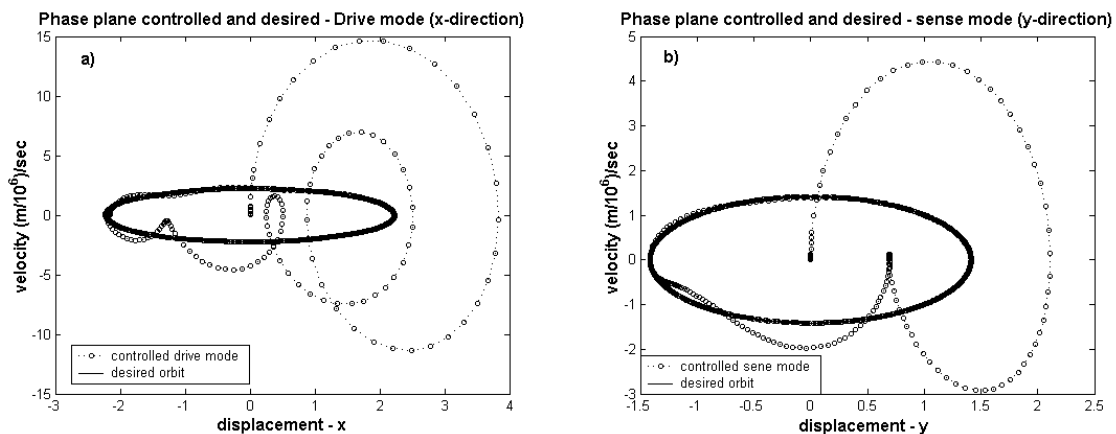


Figure 9. Phase plane and desired orbits for controlled MEMGyros. a) drive mode, and b) sense mode

Finally, Fig. 10(a,b) shows the time history of the transfer energy in the vibratory MEMGyroscope of the non-controlled and controlled system for $V_A = 50V$ and $\omega = 50KHz$. In the non-controlled system (Fig. 10a) we can observe that the energy of the drive mode isn't being transferred to sense mode by Coriolis force. It means that the most part of system energy is accumulated in the drive mode. On the other hand, (Fig. 10b) we can note the transfer of energy between drive and sense modes. Furthermore, the energy consumption of the system was controlled.

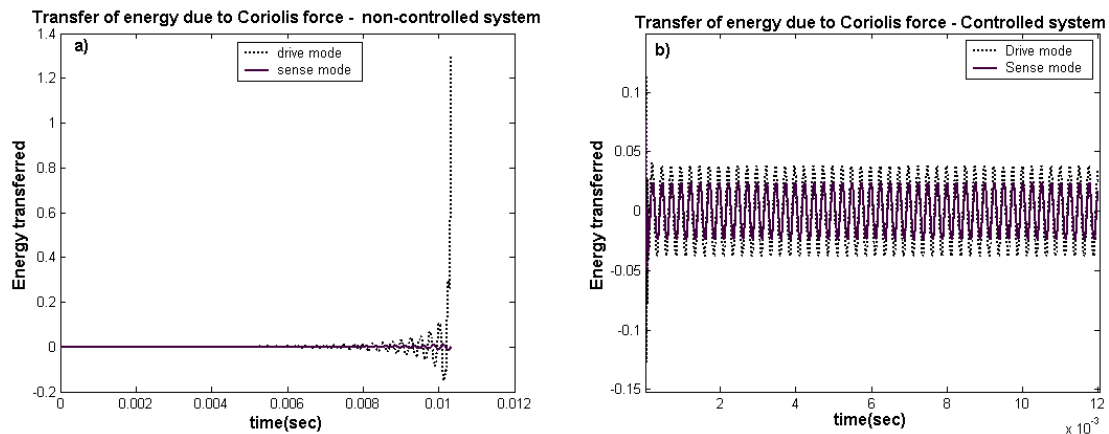


Figure 10. Transfer of energy between drive and sense modes due to Coriolis force. a) non-controlled, and b) controlled.

5. CONCLUSIONS

In this paper, was analyzed the dynamic of the mathematical model of the 2-DOF MEM vibratory gyroscope. We determined the stability diagram by numeric approximations of the Picard interaction and expansion in shifted Chebyshev polynomials which shows bifurcations boundaries of the system for the control parameters voltage e frequency. The dynamics and the transfer of energy of the system were studies for a values set of control parameters unstable of the stability diagram. Finally, dynamics and the transfer of energy were controlled to a desired periodic orbit, through a states feedback control technique based on Lyapunov-Floquet transformation. The control design reduced and controlled the transfer of energy.

6. ACKNOWLEDGMENTS

The second author thanks all the support of the Fundesp (Proc N° 00746/10-DFP) and Prope/UNESP (Programa Primeiros Projetos, Edital n° 005/2010-PROPE).

7. REFERENCES

- Adams, S.G., Bertsch, F.M., Shaw, K.A. and MacDonald, N.C. Independent Tuning of Linear and Nonlinear Stiffness Coefficients. *Journal of Microelectromechanical Systems*, 7 (2), 1998.
- Dávid, A., Sinha, S.C., “Control of Chaos in Nonlinear Systems with Time-Periodic Coefficients”. *American Control Conference*, p. 764- 768, 2000.
- Mochida, Y., Tamura, M. and Ohwada, K. A Micro Machined Vibrating Rate Gyroscope with Independent Beams for the Drive and Detection Modes. *Sensor and Actuators A (Physical)*, 80, p.170–178, 2000.
- Nayfeh, A.H, Mook, D. T. *Nonlinear oscillations*. Wiley and Sons, 1979.
- Oropeza-Ramos, L. A., Turner, K. L. Parametric Resonance Amplification in a MEMGyroscope. in *Proceedings of IEEE Sensors 2005: The Fourth IEEE Conference on Sensors*, (Irvine, California), 2005.
- Oropeza-Ramos, L. A., Burgner, C.B. and Turner, K. L. Robust micro-rate sensor actuated by parametric resonance. *Sensor and Actuators A (Physical)*, 152, p.80-87, 2009.
- Oropeza-Ramos, L. A. *Investigations on Novel Platforms of Micro Electro Mechanical Inertial Sensors: Analysis, Construction and Experimentation*. PhD Thesis, University of California, 2007.
- Peruzzi, N.J. *Nonlinear Dynamic and Control of Ideal and Non-Ideal Periodic System*. PhD Thesis, Univesity of Campinas (Unicamp), 2005. (in portuguese)
- Peruzzi, N.J.; Balthazar, J.M., Pontes, B.R., and Brasil, R.M.L.R.F. Dynamics and Control of an Ideal/ Non-Ideal Load Transportation System with Periodic Coefficients. *Journal of Computational and Nonlinear Dynamics*, v. 2, p. 32-39, 2007.
- Ruby, L. Applications of the Mathieu equation. *American Association of Physics Teachers*, 64 (1), 1994.
- Shaw, S.W., Balachandran, B. A Review of Nonlinear Dynamics of Mechanical Systems in Year 2008. *Jounal of Systema design and Dynamics*, 2 (3), 2008.
- Sinha, S.C., E.A. Butcher, “Symbolic Computation of Fundamental Solution Matrices for Linear Time-Periodic Dynamical Systems”. *Journal of Sound and Vibration*, 206(1), p61-85, 1997.
- Sinha, S.C., P. Joseph, “Control of General Dynamic Systems with Periodically Varying Parameters Via Lyapunov-Floquet Transformation”. *Journal of Dynamic, Measurement, and Control*, v.116, p.650-658, 1994.

Turner, K.L., Miller, S.A. and Hartwell, P.G. Five parametric resonances in a micro-electromechanical system *Nature*, 396, 1998.
 Yazdi, N., Ayazi, F. and Najafi, K. Micromachined Inertial Sensors. *PROCEEDINGS OF THE IEEE*, 86 (8), 1998.
 Zhang, W. Baskaran, R. and Turner, K. Effect of cubic nonlinearity on autoparametrically amplified resonant MEMS mass sensor. *Sensors and Actuators A (Physical)*, 102, p.139-150, Zhang, 2002.

8. RESPONSIBILITY NOTICE

The authors are the only responsible for the printed material included in this paper.

9. APPENDICE

The matrix A is defined:

$$A_0 = \begin{bmatrix} 0 & 0 & 1 & 0 \\ 0 & 0 & 0 & 1 \\ -\frac{2\delta_x + 15\delta_{x_3} + 9\beta_{x_3}}{2} & 0 & -\alpha_x & \gamma \\ 0 & -\frac{2\delta_y + 15\delta_{y_3}}{2} & -\gamma & -\alpha_y \end{bmatrix}$$

$$A_1 = \begin{bmatrix} 0 & 0 & 0 & 0 \\ 0 & 0 & 0 & 0 \\ -\frac{4\beta_x + 9\delta_{x_3} + 30\beta_{x_3}}{2} & 0 & 0 & 0 \\ 0 & \frac{9\delta_{y_3}}{2} & 0 & 0 \end{bmatrix}$$

$$A_2 = \begin{bmatrix} 0 & 0 & 0 & 0 \\ 0 & 0 & 0 & 0 \\ -6\delta_{x_3} & 0 & 0 & 0 \\ 0 & -6\delta_{y_3} & 0 & 0 \end{bmatrix}$$

$$A_3 = \begin{bmatrix} 0 & 0 & 0 & 0 \\ 0 & 0 & 0 & 0 \\ -4.5\beta_{x_3} & 0 & 0 & 0 \\ 0 & 0 & 0 & 0 \end{bmatrix}$$

$$A_4 = \begin{bmatrix} 0 & 0 & 0 & 0 \\ 0 & 0 & 0 & 0 \\ -6\beta_{x_3} & 0 & 0 & 0 \\ 0 & 0 & 0 & 0 \end{bmatrix}$$